Formation and characterisation of nanostructured metastable alloys

V. Pop

Faculty of Physics, Babes-Bolyai University, 3400 Cluj-Napoca, Romania

Polycrystalline solids with grain size less than 100 nm are called nanocrystalline materials. Nanocrystalline structures offer a new opportunity to improve current magnetic materials. This refers to materials such as permanent magnets, soft magnetic materials, recording media and also to materials involved in spin electronics. The properties of nanocrystalline materials are very often superior to those of conventional polycrystalline coarse grain materials. These materials can be produced using various methods and different starting phases: vapour (inert gas condensation, sputtering, plasma processing, vapour deposition), liquid (electrodeposition, rapid solidification) or solid (mechanical alloying, severe plastic deformation, spark erosion) [1-11] . A survey on mechanical alloying and rapid quenching as a method to obtain nanostructured permanent magnets and soft magnetic materials will be given. The influence of the annealing on the structure and microstructure will be also discussed. A short description concerning the synthesis of monodisperse iron-platinum nanoparticles by chemical methods will be also presented. This study does not refer to magnetic nanostructures such as dots and arrays, nanowires, multilayers or nanojonctions.

1. Introduction

The materials obtained by mechanical alloying or by very rapid solidification techniques form metastable phases. A metastable phase is a phase that does not exist in equilibrium conditions. It is not thermodynamically the most stable phase, but rather temporarily stable in certain conditions. The metastable phases correspond to a local minimum of the free energy, figure 1. The height of the energy barrier between this local energy minimum and the lowest energy minimum will give the thermodynamic stability of the metastable phase. The importance of the metastable phases for the magnetic materials applications is one of the motivations for extensive investigations of the nanostructured materials. Generally, there are three empirical requirements which must be satisfied by magnetic alloys to produce amorphous precursor:
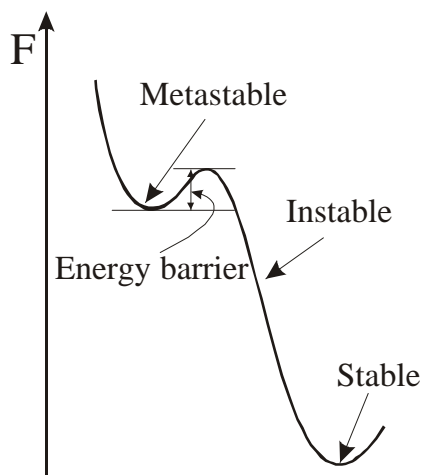
- The alloys are composed of more than ternary systems.
- The constituent alloying elements posses significantly different atom size.
- The heat formation of the amorphous alloys is negative.

The optimisation of the microstructure is the key to improve the hard magnetic properties of nanocrystalline soft magnetic materials as well as nanocomposite permanent magnets.

An example of improving the performance of hard magnetic materials by nanostructuring is *hard-soft* permanent magnet composites known as *exchange-spring magnets* [10, 12-19]. Exchange-spring magnets or spring magnets consist of nanodispersed hard and soft magnetic phases that are coupled by exchange. Spring magnets combine the high anisotropy of the hard phases with the large magnetisation found in soft magnetic phases. There are two basic parameters characterising the structure of the

Figure 1. Thermodynamical stability of a system is connected with the free energy, *F*, variation.

nanostructured materials: crystallites diameter, D, and volume fraction of nanocrystalline phases, V_{cr}. In hard magnetic nanocrystalline materials full or almost full crystallization is required. The critical dimension for the soft phase, below which the soft phase is rigidly coupled to the hard phase, is found to be roughly twice the width of domain wall in the hard phase, d_h [20]:

$$d_h = p \sqrt{A_h / K_h} \qquad (1)$$

where A_h and K_h are the exchange and anisotropy constants [21] of the hard phase, respectively. From experimental point of view, a large reversible demagnetization curve in conjunction with a strength remanence, $m_r > 0.5$ ($m_r = M_r/M_s$ where M_r is remanent magnetisation and M_s represents the saturation magnetisation), may be considered a criteria for the presence of the exchange spring mechanism.

Other nanoscale effects are exploited in soft magnetic nanostructures. Generally, the optimum mechanical and magnetic properties of the nanocrystalline soft magnetic materials are obtained for partial crystallisation materials. This means that these materials are two-phase formed; a nanocrystalline and an amorphous matrix [9]. The volume fraction of the nanocrystalline phase should be obtained so that their negative magnetostriction contribution compensates the positive magnetostriction contribution of the amorphous matrix. In the non-magnetostrictive iron nanocrystalline materials $V_{cr} \approx 70\text{-}75$ % depending on alloy composition. The nanocrystallite diameter, D, should be smaller than the magnetic exchange length, L_{ex}, in the crystalline phase to reduce the magnetocrystalline anisotropy of this phase.

$$L_{ex} = \sqrt{A / 4 p M s^2} \qquad (2)$$

According with the random anisotropy model [22] D should be smaller than 15 nm for a-Fe(Si) and a-Fe nanocrystals present in Finemet ($Fe_{73.5}Cu_1Nb_3Si_{13.5}B_9$) and Nanoperm ($Fe_{84}Zr_{3.5}Nb_{3.5}B_8Cu_1$) alloys, respectively. In crystalline classical soft materials it is well known that the coercivity increases by decreasing grain size ($1/D$ dependence); good soft magnetic properties require very large grains, $D > 100$ µm. Thus, the reduction of particle size to the regime of the domain wall width increases H_c toward a maximum given by the material anisotropy; fine particle system been compatible as hard magnetic materials. In the nanoscale region this behaviour changes. A critical grain size, D_{cr}, of about 40 nm, which divides the $H_c(D)$ behaviour in two different regions can be observed. The crystallite refinement ($D < D_{cr}$) diminishes the magnetocrystalline anisotropy due to the averaging effect of magnetisation over randomly oriented nanocrystallites, leading to a reduction of H_c. Figure 2 summarises the coercive field, H_c, behaviour in the whole range of structural correlation lengths, from atomic distances in amorphous alloys up to macroscopic grain size [11]. The permeability shows an analogous behaviour, being essentially inversely proportional to H_c. The D^6 dependence of H_c in nanometric region ($D < D_{cr}$) shows how closely hard and soft magnetic
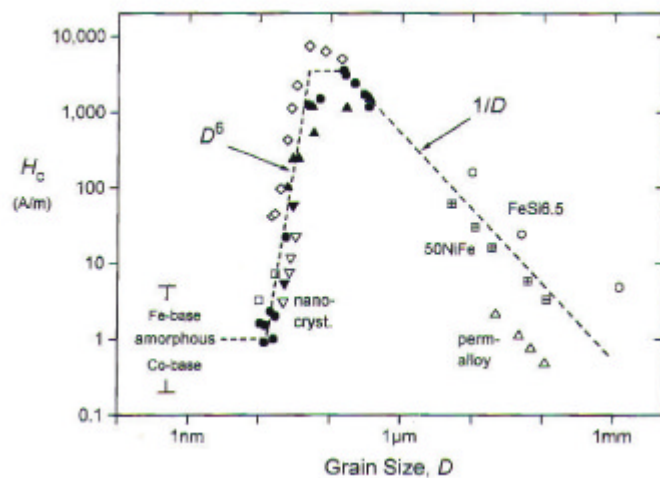

Figure 2. Coercive field, H_c, vs. grain size, D, for various soft magnetic alloys: ▲ Fe-Nb-Si-B, ● Fe-Cu-Nb-Si-B, ▼▽ Fe-Cu-V-Si-B, □ Fe-Zr-B, ◊ Fe-Co-Zr, △⊞ NiFe and ○ Fe-Si(6.5 %)

behaviour can be neighboured and decided by the correlation between grain size and ferromagnetic exchange length. Contrary to the fact that the vanish of the coercivity in superparamagnetic regime is accompanied by a low permeability, in the soft magnetic nanostructures small ferromagnetic crystallites are well coupled by exchange interactions and have simultaneously low coercivity and high permeability. Nanocrystalline materials exhibit increased strength/hardness, reduced density, reduced elastic modulus, smaller electrical conductivity, higher specific heat, higher thermal expansion coefficient, lover thermal conductivity, and superior soft magnetic properties in comparison with polycrystalline coarse grain materials.

Fe-Pt alloys with composition close to $Fe_{50}Pt_{50}$, because of their large magnetocrystalline anisotropy and good chemical stability, have been extensively studied as candidates for permanent magnets. Recently FePt films have received more attention for magnetic recording and magneto-optical recording applications [16, 23]. Their large magnetocrystalline anisotropy (10^7 J/m^3) allows for thermally stable grain diameters down to 2.8 nm. A well-organized magnetic array of such particles will allow to design magnetic devices capable of recording densities greater than 1 Tb/in^2 [24].

Rapid quenching and mechanical milling joint with appropriate heat treatments for microstructure modelling were frequently used to obtain nanocomposite soft or hard magnetic materials. Chemical synthesis of FePt nanoparticles provide a simple procedure for the preparation of the monodisperse FePt nanocrystals and FePt nanocrystals superlattice assemblies. We will develop these techniques for the fabrication of nanostructured materials.

2. Rapid quenching

By nanocrystallisation of metallic glasses, the nanocrystalline structure is obtained in two steps:
- Formation of amorphous state by rapid quenching of liquid alloy at very high cooling rate of 10^5-10^6 K/s.,
- Partial or complete crystallisation of the amorphous alloy by annealing.

We will refer mainly to rapid quenching by spin melting. Spin melting is one of the most powerful method to synthesise the amorphous, nanocrystalline and metastable phases. The liquid alloys are rapidly quenched on the surface of a cooled cooper roller, figure 3. The velocity of the roller, v_r, and the alloys composition control the formation of the amorphous, nanocrystalline and metastable phases. The grain size is dependent on v_r. Normally, the greater v_r is, the smaller grain size are formed. For a cooling rate fast enough the melt spun ribbons are amorphous. The microstructure of the melt spun ribbon can be modified by annealing. Examples of the alloys composition and main aspect of their structure are presented in Table 1.

2.1 Soft nanocrystalline magnetic materials obtained by rapid quenching

The coercivity in soft magnetic materials is strongly dependent on the crystallites (nanocrystallites) size, D, as shown in figure 2. A critical dimension $D_{cr} \approx 40$ nm divides this dependence in two very different behaviours: $H_c \sim D^6$ for $D < D_{cr}$ and $H_c \sim 1/D$ when $D > D_{cr}$. Consequently performance nanostructured magnetic materials suppose crystalline phases with nanocrystallite dimensions smaller than the critical size. A schematic illustration of the nanocrystalline structure formation in Fe-Cu-Nb-Si-B alloys is presented in figure 4.

Yoshizawa et al. [25] proposed $Fe_{73.5}Cu_1Nb_3Si_{13.5}B_9$ alloy (Finemet) with good magnetic properties: H_c = 0.5-1 A/m, m = 0.7- 1x10^5 and B_s = 1.2 T. Annealing of melt spun

Argon
Crucible
Melt
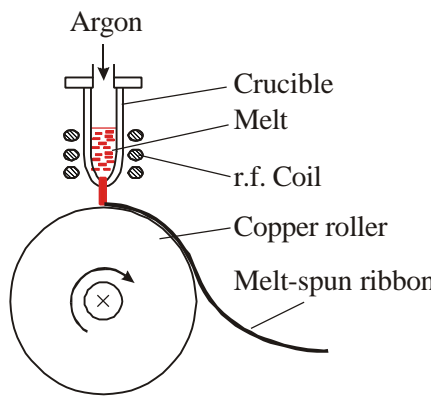r.f. Coil
Copper roller
Melt-spun ribbon

Figure 3. Schematic representation of the melt spinning technique

Table 1. General characteristics of the soft and hard magnetic materials produced by annealing of metallic glasses [9].

Nanocrystalline materials	Magnetically soft (Fe-based)	Magnetically hard (Fe-based)
Alloys	Finemet ($Fe_{73.5}Cu_1Nb_3Si_{13.5}B_9$) Nanoperm ($Fe_{84}Zr_{3.5}Nb_{3.5}B_8Cu_1$) Hitperm ($Fe_{44}Co_{44}Zr_7B_4Cu_1$)	R-Fe-B R = rare-earth e.g. $Nd_{11.8}Fe_{82.3}B_{5.9}$ $Pr_5Fe_{88}Nb_2B_5$
Structure	Nanocrystals (bcc-Fe)+ amorphous matrix	Nanocrystals $Nd_2F_{14}B$+ (Fe_3B, a-Fe, amorphous)
V_{cr} D	70–75 % $\Rightarrow \lambda_s \approx 0$[*] ≤ 15 nm $\Rightarrow \langle K \rangle \approx 0$[**]	≤ 100 % < 25 nm
Properties	High permeability, low magnetic losses	High coercivity, high remanence

[*] λ_s –saturation magnetostriction constant,

[**] $\langle K \rangle$ –averaged magnetocrystalline anisotropy

ribbons at 500-600 °C for 1 hour partially transform amorphous phases into three nanostructured components:(i) nanocrystalline a-Fe phase (D = 10-15 nm) contains 20 at% Si and few at% B; (ii) Fe-based amorphous phase, which occupies 20-30 % volume, is enriched in B and Nb and a small quantity of Si; (iii) dispersed Cu particles. The nanocrystalline phase surrounded by amorphous phase causes the lowering of the coercivity and enhances the permeability. Cu clustering serves as nuclei of a-Fe phase, while the Nb presence hinders the precipitation of hard magnetic phase Fe_2B. Both Cu and Nb impede the grain growth. The $Fe_{86-91}Zr_7B_{7-2}$ (Nanoperm) soft magnetic alloys present greater B_s (≈ 1.5 T) and similar coercivity and permeability than Finemet. These alloys are composed of nanocrystalline a-Fe

Figure 4. Schematic illustration of the formation of the nanocrystalline structure in Fe-Cu-Nb-Si-B alloys based on atom probe analysis results and TEM [11]

phase with a small volume fraction of amorphous enriched in B and Zr. The Cu addition improves the uniform dispersion of the nanophase due to Cu clustering. Si addition diminishes the magnetostriction. Partial substitution of Fe by Co is effective in increasing the B_s and Curie temperature, T_c [26]. $Fe_{44}Co_{44}Zr_7B_4Cu_1$ (Hitperm) alloy consists in nanocrystalline a-FeCo phase embedded in an amorphous phase with a ferromagnetic behaviour up to 900 °C. The Cu cluster formation in Hitperm alloys is blocked by the presence of Co as a result of the fact that Co and Cu are less repulsive than Fe and Cu [18].

Surface crystallisation is commonly observed in melt spun ribbons. It is not desirable for soft magnetic materials because it causes texture layers. Surface crystallisation was more pronounced in the free surface than in the wheel contact surface [27]. This negative effect can be diminished by mechanical grinding of the ribbons.

Principi et al. [28] show that the Cu clusters exist prior to the onset of nanocrystallisation in $Fe_{72}Cu_1Nb_{4.5}Si_{13.5}B_9$ alloy. This behaviour was excellently shown by the three-dimensional atom probe technique (3DAP) [18]. For longer annealing time, B atoms get distributed rather uniformly through the a-phase. Mössbauer measurement and magnetostrictive investigations confirm the presence of the structural interface effects in $Fe_{72}Cu_{1.5}Nb_4Si_{13.5}B_9$ nanocrystalline alloy [29]. Magnetic measurements (SQUID) and Mössbauer spectroscopy in $Fe_{90}Zr_7B_2Cu_1$ alloy show that the T_c of the residual amorphous phase follows well the increase of the amount of the a-Fe phase [30].

2.2 Hard nanocrystalline magnetic materials obtained by rapid quenching

The low remanence $M_r \approx M_s/2$ of isotropic magnets can be improved by the exchange hardening in nanoscale combinations of a soft phase and an oriented hard phase [31]. The fabrication of nanocomposite hard magnets as $Nd_2Fe_{14}B/(Fe_3B, Fe)$ and $Sm_2Fe_{17}N_3/Fe$ by melt spinning or mechanical alloying shows that it is possible to combine the high magnetisation of soft magnetic phases (Fe, Fe_3B…) and important magnetic anisotropy of rare-earth intermetallic compounds ($Nd_2Fe_{14}B$, $Sm_2Fe_{17}N_3$…). Thus, the maximum energy product of nanostructured $Sm_2Fe_{17}N_3/Fe_{65}Co_{35}$ multilayers is predicted to be as high as 1090 kJ/m^3 [32]. A useful presentation of the intrinsic magnetic properties of the main permanent magnet compounds in comparison with Fe and Co, the most common ferromagnetic elements, is given in [33].Usually the dependence of the coercivity and remanence vs. crystallite size is opposed. Consequently the crystallite dimensions will be chosen function if a maximum remanence, a strong coercivity or a maximum energy is desirable. It was given a correlation between coercivity and microstructure refinement in nanocrystalline Nd-Fe-B. The microstructure was changed by different annealing conditions [34, 35]. In $Nd_{8-19}Fe_{86-75}B_6$ melt spun ribbons, the increasing of the Nd content resulted in increasing the coercivity $_iH_c$ from about 480 to 1800 kA/m and decreasing of J_r (from about 1.1 to 0.7 T) and $(BH)_{max}$ approximately from 160 to 80 kJ/m^3. This behaviour is connected to the exchange in melt spun microstructure evidenced by TEM [36]. Additional elements as Si and Al appear to have a grain refinement effect. Ga has the similar effect at concentrations less than 2 at%. Cobalt increases T_c and improves the temperature characteristics, but in combination with Cr gives a better balance of the overall properties [36]. Cu cluster facilitate the primary precipitation of Fe_3B phase in $Nd_2Fe_{14}B/Fe_3B$ systems. Copper addition is not effective in refining the $Nd_2Fe_{14}B/a$-Fe microstructure [18]. $Sm(Co_{0.86-x}Fe_{0.1}Zr_{0.04}C_x)_{8.2}$ and $Sm(Co_{0.74-x}Fe_{0.1}Cu_{0.12}Zr_{0.04}C_x)_{8.2}$ metastable phases as TbCu7-type structure, for high temperature magnets, have been obtained by rapid solidifications and annealing [37]. The microstructure can be also controlled directly from roller speed. The remanence and coercivity of $Nd_{13.2}Fe_{79.6}Si_{1.2}B_6$ melt spun vs. roll speed are maximum at about 20 m/s [38]. High pressure has a large effect on the microstructure of a-Fe/$Sm_2(Fe,Si)_{17}C_x$ nanocomposite magnets as amorphous $Sm_8Fe_{85}Si_2C_5$ alloy is annealed at 923 K [39]. By increasing pressure from normal pressure to 6 GPa, the grain size decreases from 30.6 to 6.4 nm for the a-Fe and from 28.7 to 5.8 nm for $Sm_2(Fe,Si)_{17}C_x$ phase. This results from the fact that the pressure decreases the critical free energy required to form the crystalline nucleus and constrain its growth during the crystallisation of amorphous $Sm_8Fe_{85}Si_2C_5$. Also the volume fraction of $Sm_2(Fe,Si)_{17}C_x$ phase increases as the pressure increases. This behaviour is explained by the change of the crystallisation sequences: at low pressure a-Fe is the first crystallisation phase, while at high pressure $Sm_2(Fe,Si)_{17}C_x$ is. Praseodymium substitution by Dy in melt spun nanocomposite $Pr_2Fe_{14}B/a$-Fe has shown that the coercivity and the maximum energy product are significantly increased. Microstructure studies reveal a finer and more uniform 2:14:1/ a-Fe nanoscale microstructure in the Dy substituted samples, which leads to an enhanced exchange

coupling between the $Pr_2Fe_{14}B/a$-Fe [40]. The effect of the heating rate during annealing of $Pr_{12}Fe_{83}B_5$ melt-spun ribbons reveal that the superior magnetic properties achieved by high speed crystallisation are connected with the fine grain size and the narrow size distribution in the flakes [41]. Crystallisation of $Pr_{12}Fe_{83}B_5$ amorphous flake by the direct and indirect Joule heating improve the coercivity ($\approx$ 600 kA/m) of $Pr_2Fe_{14}B/a$-Fe nanocomposite magnets [42]. The optimum exchange coupling in $Nd_2Fe_{14}B/a$-Fe spring magnets is obtained for crystallites of about 20 nm. When the soft grain size are greater than this value, the lower degree of exchange coupling can be improved by substituting Sm for Nd, which results in an extension of the exchange coupling by reduction of the anisotropy of the hard phase. For relatively low substitution of Nd by Sm in $Nd_{4-x}Sm_xFe_{77.5}B_{18.5}$ all hard magnetic properties are enhanced [43]. The optimum microstructure of R-Fe-B (R = Nd, Pr, Dy and Tb) based nanocomposite ribbons have been found consisting of a uniform mixture of 2:14:1 and a-Fe crystallites of about 30 nm [44]. The completely amorphous Fe-rich $Nd_2Fe_{14}B$-type alloys containing 90 at% Fe were obtained by very high speed melt spinning, v_r = 80 m/s [45, 46]. The annealing influence on the microstructure was studied by X-ray diffraction (XRD), DSC and DTA diagram, Mössbauer spectrometry, VSM and SQUID magnetic measurements. The crystallites dimensions were derived from the peak broadening using the Scherrer formula. Suzuki et al. [47] propose a free energy diagram, which does not permit the appearance of $Nd_2Fe_{14}B$ phase by annealing from $Nd_2Fe_{23}B_3$ metastable phase. It has been shown that Ti and Zr additions to Nd-Fe-B alloys changes favourably the crystallisation temperature and the sequences of the phase transformation which leads to an exchange coupled magnet, even if the unwanted $Nd_2Fe_{23}B_3$ phase is present [48].

3. Mechanical alloying

Mechanical alloying, MA, is a technology that uses mechanical energy to achieve chemical reactions and structural changes. This refers especially to the formation of alloys from elemental precursors during mechanical processing. This technique allows to produce nonequilibrium structure/microstructure including amorphous alloys, extended solid solutions, metastable crystalline phases, nanocrystalline materials and quasi crystals [1-6, 17, 49]. Mechanical alloying involves the synthesis of materials by high-energy ball milling in planetary mills, vibratory mills, attritors and tumbling ball mills. The repeated collision between balls and powders with very high impact velocity, causes the powder particle to be deformed and work-hardened, figure 5. The cold welding of overlapping particles occurs between clean surfaces formed by prior fracture. The competing process of deformation,
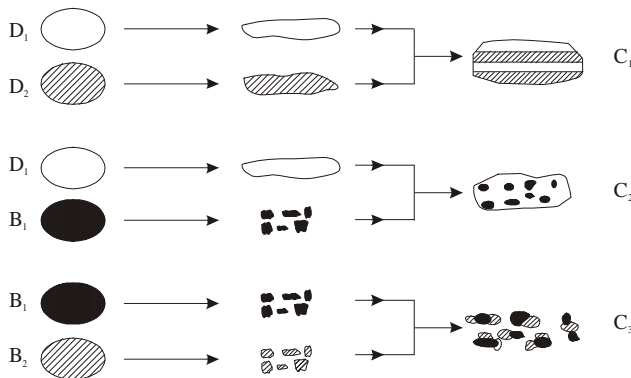

Figure 5. Scheme of the morphological transformation of the powder grains induced by milling. D – ductile powder, B – brittle powder, C – composite grains [50].
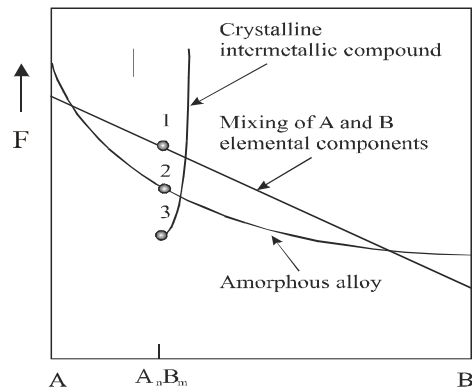

Figure 6. Schematic diagram of the free energy, F, vs. composition for binary alloys with negative energy for amorphous phase formation

fracture and welding during milling results in composition changes and microstructural refinement. *Mechanical milling,* MM, refers to the process of milling pure metals or compounds, which are in a state of thermodynamical equilibrium before milling. This process can produce disorder, amorphization and composition change. Except for the starting materials, mechanical milling is similar to the mechanical alloying. The weight rate powder/balls is usually from 1/7 to 1/10, but can be found also rates up to 1/20. Materials obtained by mechanical alloying or mechanical milling present an unusual distribution of structural defects compared with those prepared by traditional methods. As a consequence of the high number of crystalline defects it is possible to obtain amorphous alloys by mechanical alloying even for a negative energy for amorphous phase formation, figure 6 [50].

3.1 Soft nanocrystalline magnetic materials obtained by mechanical alloying

Nanocrystalline soft magnetic materials obtained by mechanical alloying present the advantage of an enforced resistivity (important in ac applications), but the significant density of defects can increase the coercivity. Consequently fabrication of nanocrystalline soft magnetic materials by MA imposes much more careful attention than the melt spinning technique. It has been shown that metastable FeCu phases can be formed by mechanical alloying. The mixture of Cu and bcc Fe are magnetically soft with low coercivity [51, 52]. The Mössbauer spectra suggest 30 % γ-Fe (fcc Fe) segregation phase in fcc Cu phase [53]. Mechanical alloying of Fe and C powder, $Fe_{100-x}C_x$ (x = 5 – 25 at%), is a way to produce magnetic nanocomposite powder (~5 μm) with crystallite size less than 5 nm [54]. Depending on *x*, the MA final product contains a-Fe, an amorphous Fe-C phase and distorted $(Fe_3C)_D$ carbide in different proportion. Annealing induces an increase in nanocrystallite size and the transition of $(Fe_3C)_D$ carbide in the non-distorted Fe_3C one. The nanocrystalline $NiFe_3O_4$ ferrite was obtained by MM. Annealing the milled $NiFe_3O_4$ has return it to a structural state similar to the bulk one, and its magnetic properties are gradually restored [55]. XRD diffractograms show that Ni and Fe_2O_3 mixture are transformed in a wüstite phase after 32 h of MA [56]. After subsequently annealed at 500-900 °C the decomposition of the wüstite phase resulted in the formation of a Ni-rich intermetallic phase and ferrite. The nanocomposite exhibit well soft magnetic properties. $Fe_{1-x}Ni_x$ alloys were prepared by MA of elemental Ni and Fe powders [57]. XRD was used for structure study. It was shown that single phase solid solution of MA samples are significantly wider than of thermodynamically stable alloys. The nanocrystalline Ni_3Fe intermetallic compound was produced by mechanical alloying of elemental Ni and Fe powders and annealing [58, 59]. The Ni_3Fe intermetallic compound was obtained after 8-10 hours of milling. The mean crystallite size of about 22 or 12 nm were obtained after 24 and respectively 52 hours of milling and 3 hours of annealing at 330 °C. The progressive synthesis of Ni_3Fe phase was checked by XRD, magnetic measurements, Mössbauer spectrometry and SEM. In order to reveal the correlation between milling time and annealing time to obtain the Ni_3Fe phase in the sample volume, a *Milling – Annealing - Transformation* (MAT) diagram was proposed [59].

3.2 Hard nanocrystalline magnetic materials obtained by mechanical alloying

At the beginning, mechanical alloying was used to produce alloy powders [60]. Mechanical alloying has been extensively applied to synthesize various metastable phases exhibiting magnetic properties. MA can be performed in free atmosphere or controlled atmosphere. For the preparation of rare-earth permanent magnetic materials, it is necessary to carry out MA in the inert atmosphere. The subsequent annealing after MA favours the formation of the metastable phases at a relevant temperature and even the equilibrium phases

at high temperatures. A good synthesis concerning the MA and properties of Nd-Fe-B magnets and Sm-Fe-X phases (X = V, Ti, Zr, N, C) with ultrahigh coercivity is given by Schultz and al. [61]. Nd-Fe-B magnets obtained by MA present properties comparable to rapid quenching materials. High energy products of 326 kJ/m^3 were reported. New hard magnetic phases were found in Sm-Fe-X alloys obtained by MA. Coercivity of 9.6-12 kA/m X=V, ThMn$_{12}$ crystal structure, 51.6 kA/m X=Ti, A$_2$ phase (Nd$_5$Fe$_{17}$ structure) [61] or 24 kA/m X=N or C [61, 62] were obtained. The as cast, annealed and MM Sm-Co-Cu-Ti magnets are compared in table 2 [63]. All samples exhibit uniaxial anisotropy with Curie temperature greater than 650 °C. A range of exchange-coupled two-phase nanocomposite hard magnetic Sm$_2$Fe$_{17}$N$_3$ and soft a-Fe were prepared by MA and subsequent annealing and nitrogenation with a view to optimize the hysteresis loop shape [64]. The main variables were the crystallisation conditions, the nitrating treatment and the chemical additives. A model of nitrogen diffusion in the two-phase nanocomposite was proposed. The Fe presence improves the nitrogenation of Sm$_2$Fe$_{17}$ phase. TEM and SEM studies evidenced that 2 at% of Zr or Ta reduce the grain size from 20-30nm to 10-20 nm, jointed by an improving of the hysteresis curve. The complete reversibility on returning to remanence was observed. Mössbauer studies reveal that the boundary phase between crystallites constitutes 15 vol% of the nanocomposite. MA of elemental powders in the composition range Sm$_x$Fe$_{100-x}$ succeed to synthesize a SmFe$_7$ phase and for higher milling time Sm$_2$Fe$_{17}$ [65]. After nitrogenation T_c raises to 480 °C. The best results are obtained in nitrided samples with x = 12.5: $_iH_c$ = 3.42 MA/m, B_r = 0.8 T and $(BH)_{max}$ = 114.4 kJ/m^3. Nitrogenation of MA Sm-Fe alloys improves the magnetic properties of Sm$_2$Fe$_{17}$C$_x$/a-Fe nanocomposites [66, 67]. Nanocomposite Sm$_2$Fe$_{17}$-Cu have been fabricated using low energy co-milling of mechanical alloyed Sm$_2$Fe$_{17}$ and Cu powders [66]. Nanocomposite magnetic properties have been controlled by milling conditions. There were produced nanocomposite Sm$_2$Fe$_{17}$-Cu with suitable magnetic properties and microstructure for high-density recording. Structural and magnetic measurements of mechanically milled SmCo$_5$ suggest that milling produces small SmCo$_5$ crystallites separated by a glassy Sm-Co interphase [67]. The volume fraction of interphase increases with additional milling. An important increasing of coercivity accompanied by remanence ratio on the order of 0.7 is induced by milling. The structure, phase transformation and magnetic properties of Sm$_y$Fe$_{100-1.5y}$C$_{0.5y}$ (y = 10 – 20) alloys prepared by MA have been studied [68]. Sm$_2$Fe$_{17}$C$_x$ structure is present for high y values and Sm$_2$Fe$_{14}$C appears for smaller y values. Sm$_2$Fe$_{17}$C$_x$ and Sm$_2$Fe$_{14}$C coexist under certain conditions. Re-milling and annealing had been developed to obtain good magnetic properties; $_iH_c$ = 640 MA/m and $(BH)_{max}$ = 84.8 kJ/m^3 in Sm$_{14}$Fe$_{79}$C$_9$ and Sm$_{20}$Fe$_{70}$C$_{10}$. High energy ball milling of Fe-Sm powders and subsequent annealing lead to the disordered SmFe$_9$ phase with TbCu$_7$-type hexagonal P6/mmm structure, which appears

as the precursor of the order R$\bar{3}$m Sm$_2$Fe$_{17}$ [69]. The effect of Si on nanocrystalline SmFe$_9$ phase with TbCu$_7$-type hexagonal P6/mmm structure was studied by HREM, XRD, Mössbauer spectrometry and magnetic measurements [70]. Si occupies 3g site and T_c is raised around 30 K compared to the equilibrium Sm$_2$(FeSi)$_{17}$ alloys. The optimal values of M_r/M_s = 0.81 and $(BH)_{max}$=54.8kJ/m^3, have been achieved for nanocomposite SmFe$_7$C$_x$/a-Fe obtained by MA [71]. Maximum specific energy of MM PrCo$_5$ powder

Table 2. Structural and room-temperature coercivity of Sm-Co-Cu-Ti intermetallic compounds [63].

Type	Compound	Structure type	m_0H_c(T)
As-cast	SmCo$_7$	TbCu$_7$ + Th$_2$Zn$_{17}$	0.05
	SmCo$_{6.7}$Ti$_{0.3}$	TbCu$_7$	0.12
	SmCo$_{6.7}$Cu$_{0.3}$	TbCu$_7$	0.10
	SmCo$_{6.7}$Ti$_{.3}$Cu$_{0.3}$	TbCu$_7$	0.15
As-cast + annealed	SmCo$_7$	CaCu$_5$ + Th$_2$Zn$_{17}$	0.12
	SmCo$_{6.7}$Ti$_{0.3}$	CaCu$_5$ + Th$_2$Zn$_{17}$	0.23
	SmCo$_{6.7}$Cu$_{0.3}$	CaCu$_5$ + Th$_2$Zn$_{17}$	0.20
	SmCo$_{6.7}$Ti0$_{.3}$Cu$_{0.3}$	CaCu$_5$ + Th$_2$Zn$_{17}$	0.26
MM + annealed	SmCo$_7$	TbCu$_7$ + Th$_2$Zn$_{17}$	0.26
	SmCo$_{6.7}$Ti$_{0.3}$	TbCu$_7$ + Th$_2$Zn$_{17}$	1.90
	SmCo$_{6.7}$Cu$_{0.3}$	TbCu$_7$ + Th$_2$Zn$_{17}$	0.70
	SmCo$_{6.7}$Ti0$_{.3}$Cu$_{0.3}$	TbCu$_7$ + Th$_2$Zn$_{17}$	2.50

have been enhanced by introducing the soft Pr_2Co_{17} phase [72]. Mechanical alloying of Co and W with $Nd_2Fe_{14}B$ influences the structure and magnetic properties of nanocomposite $Nd_2Fe_{14}B$/a-Fe magnets [73]. W addition leads to the decreasing of the grain size and remanence. Co addition determines the increase of the exchange length and the decreases of the crystallisation temperature, remanence and $(BH)_{max}$. The influence of Fe, Ti, V, Cr, Mn, Co and Al on the phase constitution and magnetic properties of Nd-Fe-B alloys was studied in MA samples [74].

3. Chemical synthesis of FePt nanoparticles

Fe-Pt alloys are an important class of materials in permanent magnet applications because of their large magnetocrystalline anisotropy and good chemical stability. Small FePt particles may be suitable for future ultrahigh density magnetic recording media applications. FePt particle thin films had mainly relied on vacuum deposition techniques. We will present some aspects concerning chemical synthesis of Fe-Pt alloys. Sun et al. [75] in order to prepare FePt nanoparticles had used a combination of oleic acid and oleyl amine to stabilise the monodisperse FePt colloids and prevent oxidation. The synthesis is based on the reduction of Pt(acac) (acac = acetylacetonate $CH_3COCHCOCH_3$) by a diol and the decomposition of $Fe(CO)_5$ in high temperature solution. HREM studies show that FePt assembly on a thermally oxidized Si substrate are well separated with no agglomeration occurring. EDX spectroscopy confirms that the average nanocrystals are slight iron rich, $Fe_{52}Pt_{48}$. Interparticle spaces are about 2 nm. A similar procedure was used to produce $Fe_{55}Pt_{45}$ nanoparticles materials [24]. Hexane dispersions of FePt and Fe_3O_4 nanoparticles with mass ratio in the range 5:1 to 20:1 were mixed under ultrasonic agitation. Three dimensional binary assembly were induced by either hexane evaporation or addition of ethanol. The size of FePt was kept at 4 nm and Fe_3O_4 was varied from 4 to 12 nm [76, 77]. The binary assemblies were converted to FePt/Fe_3Pt nanocomposites by annealing under flow of Ar +5%H_2 at 650 °C for 1h. The annealing reduces the iron oxide to iron and transforms the FePt from disordered fcc to ordered fct structure with high magnetocrystalline anisotropy. The partial interdiffusion between Fe and FePt creates a new fcc phase, Fe_3Pt, which is magnetically soft with a high magnetisation.

References

[1] C. C. Koch, J. D. Whittenberger, Intermetallics 4 (1996) 339.
[2] G. Cocco, G. Mulas, L. Schif.ni, Mater. Trans. JIM 36 (1995) 150.
[3] P.H. Shingu, K.N. Ishihara, Mater. Trans. JIM 36 (1995) 96.
[4] E. Gaffet, M. Abdellaoui, N. Malhouroux-Gaffet, Mater. Trans. JIM 36 (1995) 198.
[5] R. Watanabe, H. Hashimoto, G.G. Lee, Mater. Trans. JIM 36 (1995) 102.
[6] T.H. Courtney, Mater. Trans JIM 36 (1995) 110.
[7] J. I. Martin, J. Nogues, Kai Liu, J. L. Vicent, I. K. Schuller, J. Magn. Magn. Mater. 256 (2003) 449
[8] C. Suryanarayana, Int. Mat. Rev. 40 (1995) 41.
[9] T. Kulik, J. Non Crystalin Solids 287 (2001) 145.
[10] K.H.J. Buschow, Handbook of Mag. Mater., Ed. K.H.J. Buschow, Vol 10 (1997) 463.
[11] G. Herzer, Handbook of Mag. Mater., Ed. K.H.J. Buschow, Vol 10 (1997) 415.
[12] R. Coehoorn, D. B. de Mooij, C. De Waard, J. Magn. Magn. Mater. 80 (1989) 101.

[13] R. Skomski, J. Phys. : Condens. Matter. 15 (2003) R841.

[14] R. Skomski, J. M. D. Coey, *Permanent Magnetism*, 1999 (Bristol: Institute of Physics Publishimg).

[15] E. F. Kneller, R. Hawig, IEEE Trans. Mag. 27 (1991) 3588.

[16] G. C. Hadjipanayis, J. Magn. Magn. Mater. 200 (1999) 373.

[17] Z. D. Zhang, W. Liu, J. P. Liu, D. J. Sellmyer, J. Phys. D: Appl. Phys. 33 (2000) R217.

[18] K. Hono, D. H. Ping, Y. Q. Wu, Proceedings 22nd Ris$\varnothing$ Int. Symp. On Material Science, 2001 Roskilde, Denmark.

[19] J. Petzold, J. Magn. Magn. Mater. 242-245 (2002) 84.

[20] E. E. Fullerton, J. S. Jiang, S. D. Bader, J. Magn. Magn. Mater. 200 (1999) 392.

[21] C. Kittel, Rev. Mod. Phys. 21 (1949) 541.

[22] G. Herzer, IEEE Trans. Magn. MAG-25 (1989) 3327; IEEE Trans. Magn. MAG-26 (1990) 1397.

[23] J. P. Liu, Y. Liu, C. P. Luo, Z. S. Zhan, D. J. Sellmyer, Appl. Phys. Lett. 72 (1998) 483.

[24] S. Sun, E. E. Fullerton, D. Weller, C. B. Murray, IEEE Trans. Magn. 37 (2001) 1239.

[25] Y. Yoshizawa, S. Oguma, K. Yamauchi, J. Appl. Phys., 64 (1988) 6044.

[26] M.A. Willard, M. Q. Huang, D. E. Laughlin, M. E. McHenry, J. O. Cross, V. G. Harris, J. Appl. Phys., 85 (1999) 4421.

[27] Y. Q. Wu, T. Bitoh, K. Hono, A. Makino, A. Inoue, Acta Mater. 2001.

[28] G. Principi, A. Maddalena, M. Meyer, S. Dal Toé, A. Gupta, P, Sharma, B. A. Dassannacharya, N. Paul, S. Bernstorff, H. Amenitsch, ICM Rome 2003, be published in J. Magn. Magn. Mater.

[29] T. Szumiata, K. Brzozka, M. Gawronski, B. Gorka, J. S. Blazquez-Gamez, T. Kulik, R. Zuberek, A. Slawska-Waniewska, ICM Rome 2003, be published in J. Magn. Magn. Mater.

[30] L. F. Kiss, D. Kaptas, J. Balogh, J. Gubicza, T. Kemeny, I. Vincze, ICM Rome 2003, be published in J. Magn. Magn. Mater.

[31] R. Skomski, J. M. D. Coey, Phys. Rev. B48 (1993) 15812.

[32] R. Skomski, J. Appl. Phys. 76 (1994) 7059

[33] J. M. D. Coey, Solid State Commun. 102 (1997) 101.

[34] E. Burzo, O. Ersen and V. Pop, Balkan Physics Letters Vol. 5 Suppl. (1997) 1243.

[35] E. Burzo, H. Chiriac, O. Ersen, V. Pop, Proc. Travaux du deuxième atelier scientifique Franco-Canadiano-Roumain. Matériaux magnétique. 17-19 Mai 1999 Bucarest, Roumanie, pag. 85-90.

[36] H. A. Davies, J. Magn. Magn. Mater. 157-158 (1996) 11.

[37] S. S. Makridis, G. Litsardakis, K. G. Efthimiadis, S. Höfinger, J. Fidler, D. Niarchos, ICM Rome 2003, be published in J. Magn. Magn. Mater.

[38] H. A. Davies, *Nanophase Materials*, G. C. Hadjipanayis and R. W. Siegel (eds), 1994 Kluwer Academic Publishers, p. 675.

[39] X. Y. Zhang, J. W. Zhang, W. K. Wang, J. Appl. Phys. 89 (2001) 477.

[40] Z. Chen, H. Okumura, G. C. Hadjipanayis, Q. Chen, J. Appl. Phys. 89 (2001) 2299.

[41] H. Fukunaga, K. Tokunaaga, J. M. Song, IEEE Tran. Magn. 38 (2001) 2970.

[42] H. Fukunaga, A. Tagawa, M. Nakano, ICM Rome 2003, be published in J. Magn. Magn. Mater.

[43] Q. F. Xiao, T. Zhao, Z. D. Zhang, E. Brück, K. H. J. Buschow, F. R. DeBoer, J. Magn. Magn. Mater. 223 (2001) 215.

[44] L. Withanawasam, A. S. Murphy, G. C. Hadjipanayis, R. F. Krause, J. Appl. Phys. 76 (1994) 7065.

[45] D. Negri, A. R. Yavary, M. Vasquez, A. Hernando, A. Deriu, T. Hopfinger, Mat. Sci. Forum 235-238 (1997) 807.

[46] T. Hopfinger, A. R. Yavary, D. Negri, J. Alonso, A. Hernando, J. Magn. Magn. Mater. 164 (1996) L7.

[47] K. Suzuki, J. M. Kadogan, M. Uehara, S. Hirosawa, H. Kanekiyo, J. Appl. Phys. 85 (1999) 5914.

[48] A. Jianu, M. Valeanu, D. P. Lazar, F. Lifei, C. Bunescu, V. Pop, ICM Rome 2003, be published in J. Magn. Magn. Mater.

[49] L. Shultz, Philos. Mag. B61 (1990) 453; L. Shultz, J. Wecker, Mater. Sci. Eng. 89 (1988) 127.

[50] V. Pop, I. Chicinas, N. Jumate, *Material Physics. Experimental Methods* , Presa Universitara Clujeana, 2001 (Romanian).

[51] A. R. Yavary, P. J. Desre, T. Benameur, Phys. Rev. Lett. 68 (1992) 2235.

[52] T. Ambrose, A. Gavrin, C. L. Chien, J. Magn. Magn. Mater. 124 (1993) 15.

[53] A. Hernando, P. Crespo, J. M. Barandiaran, A. Garcia Escorial, R. Yavary, J. Magn. Magn. Mater. 124 (1993)5.

[54] E. P. Yelsukov, A. I. Ul'yanov, A.V. Zagainov, N. V. Arsent'yeva, J. Magn. Magn. Mater. 258-259 (2003) 513.

[55] V. Sepelak, D. Baabe, D. Mienert, D. Schultze, F. Krumeich, F. J. Litterst, K. D. Becker, J. Magn. Magn. Mater. 257 (2003) 377.

[56] Y. Shi, J. Ding, S. L. H. Tan, Z. Hu, J. Magn. Magn. Mater. 256 (2003) 13.

[57] V. V. Tcherdyntsev, S. D. Kaloshkin, Y. A. Tomilin, E. V. Shelekhov, Yu. V. Baldokhin, NanoStructure Mat. 12 (1999) 139.

[58] I. Chicinas, V. Pop, O. Isnard, J.M. Le Breton, J. Juraszek, Journal of Alloys and Compounds 352 (2003) 34.

[59] V. Pop, O. Isnard, I. Chicinas, Journal of Alloys and Compounds (2003) in press.

[60] J. J. Benjamin, Metall. Trans. 1 (1970) 2067; Sci. Am. 234 (1976) 40.

[61] L. Schultz, K. Schnitzke, J. Wecker, M. Katter, C. Kuhrt, J. Appl. Phys. 70 (1991) 6339.

[62] P. A. P. Wendhausen, B. Gebel, D. Eckert, K. H. Muller, J. Appl. Phys. 75 (1994) 6019.

[63] M. Venkatesan, C. Jiang, J. M. D. Coey, J. Magn. Magn. Mater. 242-245 (2002) 1350.

[64] K. O'Donnell, J. M. D. Coey, J. Appl. Phys. 81 (1997) 6311.

[65] L. Wei, W. Qun, X. K. Sun, Z. Xin-guo, Z. Tong, Z. Zhi-dong, Y. C. Chuang, J. Magn. Magn. Mater. 131 (1994) 413.

[66] J. X. Zhang, L. Bessais, C. Djega-Mariadassou, E. Leroy, A. Percheron-Guegan, Y. Champion, Appl. Phys. Lett. 80 (2002) 1960.

[67] D. L. Leslie-Pelecky, R. L. Schalek, Phys. Rev. B59 (1999) 457.

[68] D. Geng, Z. Zhang, B. Cui, Z. Guo, W. Liu, X. Zhao, T. Zhao, J. Liu, J. Alloys and Compounds 291 (1999) 276.

[69] C. Djega-Mariadassou, L. Bessais, J. Magn. Magn. Mater. 210 (2000) 81.

[70] A. Nandra, L. Bessais, C. Djega-Mariadasssou, E. Burzo, ICM Rome 2003, be published in J. Magn. Magn. Mater.

[71] D. Geng, Z. Zhang, B. Cui, W. Liu, X. Zhao, M. Yu, J. Magn. Magn. Mater. 224 (2001) 33.

[72] Z. Chen, Y. Zhang, G. C. Hadjipanayis, J. Magn. Magn. Mater. 219 (2000) 178.

[73] C. You, X. K. Sun, W. Liu, B. Cui, X. Zhao, Z. Zhang, J. Phys. D.: Appl. Phys. 33 (2000) 926.

[74] W. Liu, Z. D. Zhang, J. P. Liu, X. K. Sun, D. J. Sellmyer, X. G. Shao, J. Magn. Magn. Mater. 221 (2000) 278.

[75] S. Sun, C. B. Murray, D. Weller, L. Folks, A. Moser, Science 287 (2000) 1989.

[76] H. Zeng, J. Li, J. P. Liu, Z. L. Wang, S. Sun, Nature 420 (2002) 395.

[77] D. J. Sellmyer, Nature 420 (2002) 374.